

Supplementary Table 2. Primer list for quantitative RT-PCR

ALB	F 5'-AGTGTGTGTCAGAGGCTGAC-3'	MRP3	F 5'-ACCAGGAGGACCATGAAGC-3'
	R 5'-TTCTCCTTCACACCATCAAGC-3'		R 5'-TGTGGGTGCTGAGTGTGTCT-3'
β -actin	F 5'-AAGGCCAACCGTGAAAAGAT-3'	c-Myc	F 5'-CTTCTCTCCTCCTCGGACTC-3'
	R 5'-GTGGTACGACCAGAGGCATAC-3'		R 5'-CCTCATCTTCTTGCTCTTCTCA-3'
CK19	F 5'-TGACCTGGAGATGCAGATTG-3'	Notch1	F 5'-CTGGACCCCATGGACATC-3'
	R 5'-CCTCAGGGCAGTAATTCCTC-3'		R 5'-AGGATGACTGCACACATTGC-3'
CPS1	F 5'-GACACCACTGCCGAGAC-3'	Notch2	F 5'-TGCCTGTTTGACAACCTTGAGT-3'
	R 5'-CAGCAGACCTGCCACCTT-3'		R 5'-GTGGTCTGCACAGTATTTGTCAT-3'
CyclinD1	F 5'-TTTCTTTCCAGAGTCATCAAGTGT-3'	Sox9	F 5'-CAGCAAGACTCTGGGCAAG-3'
	R 5'-TGACTCCAGAAGGGCTTCAA-3'		R 5'-TCCACGAAGGGTCTCTTCTC-3'
G6Pase	F 5'-TCTGTCCCGGATCTACCTTG-3'	TAT	F 5'-GGAGGAGGTCGCTTCCTATT-3'
	R 5'-GAAAGTTTCAGCCACAGCAA-3'		R 5'-GCCACTCGTCAGAATGACATC-3'
Hes-1	F 5'-TGCCAGCTGATATAATGGAGAA-3'	TGF α	F 5'-CCTGGTGGTGGTCTCCATT-3'
	R 5'-CCATGATAGGCTTTGATGACTTT-3'		R 5'-CAGTGTTTGC GGAGCTGA-3'
HNF4 α	F 5'-TCCTGCAGGCAGAGGTTT-3'	TO	F 5'-TCCAGGGAGCACTGATGATA-3'
	R 5'-CGCCATTGATCCCAGAGA-3'		R 5'-CTGGAAAGGGACCTGGAATC-3'
HNF1 β	F 5'-AGAGCCCAGGCAGTCACA-3'	Wnt4	F 5'-GCGTAGCCTTCTCACAGTCC-3'
	R 5'-GGGGTTCCTGCTTATGTGC-3'		R 5'-CGCATGTGTGTCAAGATGG-3'
Jagged1	F 5'-GAGGCGTCCTCTGAAAAACA-3'	Wnt5a	F 5'-TGAAGCAGGCCGTAGGAC-3'
	R 5'-ACCCAAGCCACTGTTAAGACA-3'		R 5'-AGCCAGCACGTCTTGAGG-3'
Jagged2	F 5'-CGTCATTCCCTTTAGTTTCG-3'		
	R 5'-CCTCATCTGGAGTGGTGTCA-3'		

ALB, albumin; CPS1, carbamoyl phosphate synthetase 1; CK19, Cytokeratin 19;

G6Pase, glucose-6-phosphatase; HNF4 α , hepatocyte nuclear factor 4 α ; MRP3,

multidrug resistance-associated protein 3; TAT, tyrosine aminotransferase; TGF α , Transforming growth factor α ; TO, tryptophan-2,3-oxygenase; F, forward primer; R, reverse primer.

Accepted Article

Supplementary Table 3. List of antibodies for immunostaining

Primary antibodies	Species	Sources (Catalog#)	Dilution
Cytokeratin19	Rabbit	produced by Dr. A. Miyajima (Tokyo University) ⁶	2000
Entactin	Rat	Abcam (ab44944)	500
Hes1	Rabbit	Produced by Dr. T. Sudo (Toray Industries, Kamakura, Japan) ⁷	40,000
HNF1 β	Rabbit	Santa Cruz (sc-22840)	250
HNF4 α	Goat	Santa Cruz (sc-6556)	500
PCNA	Mouse	Cell Signaling (2586)	100
Phospho-CaMKII α (Thr286)	Rabbit	Cell Signaling (3361)	100
Phospho-PKCa β II (Thr638/641)	Rabbit	Cell Signaling (9375)	100
p75 NTR	Rabbit	Abcam (ab8875)	100

HNF, Hepatocyte nuclear factor; CaMKII, Calcium/calmodulin-dependent kinase II;

NTR, Neurotrophin receptor, PKC, Protein kinase C.

Supplementary Table 4. List of antibodies for immunoblots

Primary antibodies	Species	Sources (Catalog#)	Dilution
Albumin	Goat	Bethyl (A90-134A)	2000
AFP	Rabbit	Thermo (RB-365)	200
Phospho- β -catenin (Ser552)	Rabbit	Cell Signaling (9566)	1000
CaMKII	Rabbit	Cell signaling (3362)	1000
CaMKII α	Mouse	Santa Cruz (sc-32288)	100
Phospho-CaMKII α (Thr286)	Mouse	Abcam (ab2724)	1000
Cytokeratin19	Rabbit	produced by Dr Miyajima ⁶	100000
p53	Rabbit	Cell Signaling (2524S)	1000
Phospho-p53 (Ser15)	Rabbit	Cell Signaling (9284)	1000
PCNA	Mouse	Cell Signaling (2586)	2000
PKC α	Rabbit	Cell Signaling (2056)	1000
Phospho-PKC α β II (Thr638/641)	Rabbit	Cell Signaling (9375)	1000
Rac1	Rabbit	Cell Signaling (2465)	1000
Phospho-Rac1 (Ser71)	Rabbit	Cell Signaling (2461)	1000
β -actin	Mouse	Sigma (A5441)	5000

AFP; α -fetoprotein; CaMKII, Calcium/calmodulin-dependent kinase II; PCNA, Proliferating cell nuclear antigen; PKC, Protein kinase C.

Supplementary Table 5. Representative genes in cDNA microarray analysis**Down-regulated genes in Wnt5a KO mice**

Entrez ID	Symbol	Description	KO/WT Ratio
NM_032541	Hamp1	hepcidin antimicrobial peptide 1	0.21
NM_183257	Hamp2	hepcidin antimicrobial peptide 2	0.23
XM_130814	NP_083982.1	carboxypeptidase B1	0.25
NM_008218	Hba-a1	hemoglobin alpha, adult chain 1	0.27
NM_010544	Ihh	Indian hedgehog	0.31
NM_009606	Acta1	actin, alpha 1, skeletal muscle	0.32
-	Slc15a2	solute carrier family 15 (H ⁺ /peptide transporter), member 2	0.34
-	Hbb-b1	hemoglobin, beta adult major chain	0.37
NM_023637	Sars2	seryl-aminoacyl-tRNA synthetase 2	0.38
NM_013465	Ahsg	alpha-2-HS-glycoprotein	0.38

Up-regulated genes in Wnt5a KO mice

Entrez ID	Symbol	Description	KO/WT Ratio
NM_134144	Cyp2c50	cytochrome P450, family 2, subfamily c, polypeptide 50	10.15
NM_009850	Cd3g	CD3 antigen, gamma polypeptide	9.90
-	IGKV7-33	Immunoglobulin Kappa light chain V gene segment	8.99
NM_010666	Krt27	keratin 27	8.95
NM_008241	Foxg1	forkhead box G1	7.49
NM_146662	Olf365	olfactory receptor 365	7.48
-	Syce1	synaptonemal complex central element protein 1	7.48
NM_183427	Gla2	glycine receptor, alpha 2 subunit	7.43
NM_010001	Cyp2c37	cytochrome P450, family 2, subfamily c, polypeptide 37	7.36
NM_011260	Reg3g	regenerating islet-derived 3 gamma	7.05

Supplementary Figure Legends**Supplementary Figure 1. Expression analysis of Frizzled (Fzd)-family genes using**

densitometry. Expression levels of Fzd-family genes (Fig. 1C) were quantified using densitometry. Values represent the ratio relative to the density of Lane 1 (hepatoblasts).

Lane 1, 2 and 3 represent CD45⁻Ter119⁻Dlk^{high} cells (hepatoblasts) in E14.5 Liver, CD45⁺Ter119⁺ cells (hematopoietic cells) in E14.5 Liver, and adult hepatocytes, respectively.

Supplementary Figure 2. Phenotype of E18.5 Wnt5a deficient (KO) mice.

(A) Representative macroscopic view of E18.5 Wnt5a KO (left) and wild type (WT, right) embryos. (B) Representative macroscopic view of E18.5 Wnt5a KO (upper) and WT livers (lower). (C) Analysis on ratio of liver weight (left panel) and liver:body weight (right panel). Values represent the ratio relative to the mean for the livers in WT mice. Although the average liver weight in Wnt5a KO E18.5 fetal mice was significantly lower than in WT littermates, the average ratio of liver:body weight in Wnt5a KO mice was almost equal to that in littermate WT mice. Bars in dot-plot graphs represent mean \pm SD of values shown. *p < 0.001.

Supplementary Figure 3. Expression analysis of molecules related to biliary

differentiation in Wnt5a KO livers. (A) Quantitative RT-PCR analysis of the *Notch1*, *Notch2*, *Jagged1*, *Jagged2*, *Hes1*, *CK19*, and *hepatic nuclear factor (HNF)1 β* in E16.5 fetal livers. Values represent the ratio relative to the mean for the livers of WT mice. Steady-state levels of Notch1, Notch2, and Jagged1 in Wnt5a KO livers were significantly higher than in littermate WT livers. (B) Immunohistological analysis of Hes1 in E18.5 livers. Left 2 panels; immunostaining of Hes1 (green) in E18.5 livers. Right panel; number of Hes1⁺ cells in 10 random fields examined in WT and Wnt5a KO livers. Numbers of Hes1⁺ cells were significantly higher in Wnt5a KO livers relative to WT mice, indicating that numbers of Notch-activated cells were increased in Wnt5a KO livers. Bars in dot-plot graphs represent mean \pm SD of values shown. The result is representative of 3 independent experiments. *p < 0.01. **p < 0.05. PV: portal vein. Scale bars: 50 μ m.

Supplementary Figure 4. Expression analysis of proliferation markers in Wnt5a

KO livers. (A) Quantitative RT-PCR analysis of the *cyclin D1*, *c-Myc*, and *transforming growth factor (TGF) α* in E16.5 and E18.5 fetal livers. Values represent the ratio relative to the mean for the livers of WT mice. Expression levels of these genes in Wnt5a KO livers were almost equal to that in WT livers. (B) Immunoblot analysis of Proliferating cell nuclear antigen (PCNA) in E16.5 WT and Wnt5a KO livers (left

panel). Mice 1-4 and Mice 5-8 are E16.5 WT and Wnt5a KO, respectively. Values represent the ratio relative to the mean for the livers of WT mice (right panel). PCNA production in Wnt5a KO livers was almost equal to that in WT livers. PTC: positive control. (C) Immunohistological analysis of PCNA and CK19 in E18.5 livers. Left 2 panels; immunostaining of PCNA (green) and CK19 (red) in E18.5 livers. Right panel; number of PCNA⁺CK19⁺ cells in 10 random fields examined in WT and Wnt5a KO livers. Numbers of PCNA⁺CK19⁺ cells in Wnt5a KO livers were almost equal to those in WT mice. Bars in dot-plot graphs represent mean \pm SD of values shown. The result is representative of 3 independent experiments. PV: portal vein. Scale bars: 20 μ m.

Supplementary Figure 5. Expression analysis and cDNA microarray analysis of

molecules in Wnt5a KO livers. (A) Quantitative RT-PCR analysis of the hepatocyte differentiation markers, albumin (ALB) and hepatocyte nuclear factor (HNF) 4 α , is depicted as the ratio of ALB and HNF4 α copy number in E16.5 Wnt5a KO livers relative to WT livers, respectively. Steady-state levels of ALB and HNF4 α mRNA in Wnt5a KO livers were almost equal to that in WT livers. (B) Expressions of ALB, HNF4 α , glucose-6-phosphatase (G6Pase), tyrosine amino transferase (TAT), and carbamoyl phosphate synthetase 1 (CPS1) in E18.5 fetal livers. Values represent the ratio relative to the mean for the livers of WT mice. Steady-state levels of the hepatic

markers in Wnt5a KO livers were almost equal to that in WT livers. Bars in dot-plot graphs represent mean \pm SD of values shown. The result is representative of 3 independent experiments. (C) Hierarchical cluster analysis of up- or down-regulated genes based on cDNA microarray using liver tissues of E18.5 WT or Wnt5a KO mice (left panel). WT/KO normalized ratios >2.0 or <0.5 were defined as up- or down-regulated genes, respectively. Pathway analysis indicated the up- or down-regulated pathways in E18.5 Wnt5a KO livers (right panel).

Supplementary Figure 6. Representative views of bile duct-like cysts in

three-dimensional culture of a hepatic progenitor cell line (HPPL). We categorized HPPL-derived colonies into one of three classes, (A) colonies without clear lumina, (B) small cysts (50-100 μm diameter with clear lumina) and (C) large cysts (>100 μm diameter with clear lumina). Immunocytostaining analysis showed that colonies without clear lumina produced both the hepatocytic marker ALB and the biliary marker CK19 as previously described.⁸ Cells in the luminal walls of small and large cyst, in contrast, produced the biliary marker CK19 alone, indicating their differentiation to a cholangiocyte lineage. The number of cells in luminal walls judged under confocal lasermicroscope was ~ 20 -50 cells/round and >50 cells/round in small and large cysts, respectively. Scale bars: 100 μm .

Supplementary Figure 7. Analysis of HPPL-derived cysts treated with Wnt5a

inhibitors. (A) Quantitative RT-PCR analysis of *Wnt5a* in primary CD45⁻ Ter119⁻ Dlk^{high} cells of E14.5 WT fetal livers (hepatoblasts, Dlk^{high}) and HPPL cultured on laminin-coated dish (HPPL). Values represent the ratio relative to the mean for the Dlk^{high} cells. *Wnt5a* is expressed in hepatoblasts and HPPL. (B) Numbers of bile duct-like cysts derived from the HPPL in 5 random fields per well in cultures supplemented with either vehicle (DMSO), Wnt5a inhibitor (100 μ M Box5), both Wnt5a inhibitor plus 100 ng/ml recombinant Wnt5a, or 100 ng/ml recombinant Wnt5a. Cultures with Wnt5a inhibitor resulted in a significant increase in total numbers of bile-duct like cysts derived from HPPL relative to vehicle-only controls, and blocked the effect of Wnt5a supplementation. (C) Quantitative RT-PCR analysis of the *HNF1 β* , *Sox9*, *Notch1*, *Notch2*, *Jagged1*, *Jagged2*, *MRP3*, *HNF4 α* , *cyclin D1*, and *c-Myc* in HPPL-derived cysts treated with control goat IgG or anti-Wnt5a Ab. Values represent the ratio relative to the mean for the samples of control Ab. Expression levels of HNF1 β , Sox9, and Notch2 were significantly upregulated in cultured cells supplemented with anti-Wnt5a Ab relative to control Ab. (D) Immunoblot analysis of CK19, ALB, AFP, and PCNA in HPPL-derived cysts treated with anti-Wnt5a Ab. Lane 1-3 and Lane 4-6 are control IgG-supplemented controls and anti-Wnt5a Ab-supplemented samples,

respectively. Protein levels of CK19, ALB, AFP, and PCNA did not change. Bars represent mean \pm SD of values. The result is representative of 3 independent experiments. * $p < 0.05$.

Supplementary Figure 8. Expression analysis of molecules in HPPL-derived cysts

treated with vehicle (DMSO) or CaMKII inhibitor (KN62). Quantitative RT-PCR

analysis of the *CK19*, *HNF1 β* , *Notch1*, *Notch2*, *Jagged1*, *Jagged2*, *ALB*, *HNF4 α* , *cyclin*

D1, *c-Myc*, and *TGF α* in HPPL-derived cysts treated with vehicle (DMSO) or CaMKII

inhibitor (KN62). Values represent the ratio relative to the mean for the samples of

vehicle-only controls. Bars represent mean \pm SD of values. The result is

representative of 3 independent experiments.

Supplementary Figure 9. Phosphorylation of CaMKII α and PKC in developing

liver and primary hepatic stem/progenitor cells. (A) Immunoblot analysis of

phosphorylated CaMKII α (p-CaMKII α) and phosphorylated PKC (p-PKC) in

embryonic E14.5, 16.5, 18.5, postnatal P1, P7, and P14 WT livers. Homogenate of

whole E14.5 embryo served as a positive control (PTC). Fluorescence of bands

corresponding to of CaMKII α and p-CAMKII α is increased gradually during liver

development. (B) Analysis of FACS-purified primary hepatic stem/progenitor cells

immunostained with anti-p-CaMKII α or anti-p-PKC antibodies (red signals). Nuclei were counterstained with DAPI (blue signals). Non-specific rabbit IgG was used as an isotype control. Scale bars: 100 μ m.

Supplementary Figure 10. Quantitative analysis of immunoblots using

densitometry. (A) Immunoblot analysis of phosphorylated CaMKII α (p-CaMKII α) and total CaMKII protein in HPPL after Wnt5a stimulation (shown in Fig. 6A) was

quantified using densitometry. Values represent the ratio relative to the density of p-CaMKII α (red bars) or CaMKII (black bars) in HPPL at pretreatment. Wnt5a

stimulation increased both CaMKII and p-CaMKII α with the levels peaking 3 hours after Wnt5a supplementation and then decreasing to baseline levels after 12 hours. (B)

Ratios of p-CaMKII α /CaMKII quantified by densitometry increased, peaking 3 hours after Wnt5a supplementation. (C) Immunoblot analysis of phosphorylated PKC

(p-PKC) and total PKC α protein in HPPL after Wnt5a stimulation (shown in Fig. 6A) was quantified using densitometry. Values represent ratios of p-PKC/PKC α relative to

the value in HPPL at pretreatment. (D) Immunoblot analysis of phosphorylated Rac1

(p-Rac1) and total Rac protein in HPPL after Wnt5a stimulation (shown in Fig. 6A) was quantified using densitometry. Values represent ratios of p-Rac1/Rac1 relative to the

value in HPPL at pretreatment. (E) Immunoblot analysis of p-CaMKII α in E16.5 Wnt5a

KO and littermate WT fetal livers (shown in Fig. 6D) was quantified using densitometry.

Levels of p-CaMKII α were significantly lower in Wnt5a KO relative to WT fetal livers.

Values represent the ratio relative to the mean density for WT mice. Bars in dot-plot

graphs represent mean \pm SD of 5 mice shown. The result is representative of 3

independent experiments. *p =0.008.

Supplementary Figure 11. Analysis of HNF1 β , p75NTR, and p-CaMKII in Wnt5a

KO livers. (A) Immunostaining of HNF1 β (green) and HNF4 α (red) in E14.5 livers.

Nuclei were stained with DAPI (blue). HNF1 β was not detected in both E14.5 WT and

Wnt5a KO livers. (B) Immunostaining of p75NTR (green) in E18.5 livers. Nuclei were

stained with DAPI (blue). Cells with p75NTR were detected in E18.5 Wnt5a KO and

littermate WT livers. Scale bars: 50 μ m.

Supplementary Figure 12. Pancreas and kidney in Wnt5a KO mice. (A).

Representative stereoscopic views of pancreas and kidney in E18.5 Wnt5a KO and

littermate WT mice. White dashed lines show the margins of kidneys. Scale bars: 1 mm.

(B) Representative images depicting pancreas and kidney tissues in E18.5 Wnt5a KO

and littermate WT mice stained with hematoxylin and eosin.

Supplementary Figure 13. Analysis of Wnt4a, phosphorylated β -catenin, and**phosphorylated p53.** (A) Expression of *Wnt4* in fetal livers of E16.5 Wnt5a KO andlittermate WT mice. Quantitative RT-PCR analysis of *Wnt4* is depicted as the ratio of*Wnt4* copy number in E16.5 Wnt5a KO livers relative to WT livers. Bars in dot-plotgraphs represent mean \pm SD of 6 mice shown. The result is representative of 3independent experiments. * $p=0.02$. (B) Immunoblot analysis of phosphorylated β -catenin (p- β -catenin, activated β -catenin), phosphorylated p53 (p-p53, stabilized p53),

and total p53 protein in HPPL at pretreatment (0), and then 1, 3, 6 and 12 hours after

stimulation by Wnt5a. (C) Immunoblot analysis of p- β -catenin in supplementary Figure

13B was quantified using densitometry. Values represent the ratio relative to the density

of p- β -catenin in HPPL at pretreatment. (D) Immunoblot analysis of p-p53 and total p53

in supplementary Figure 13B was quantified using densitometry. Values represent ratios

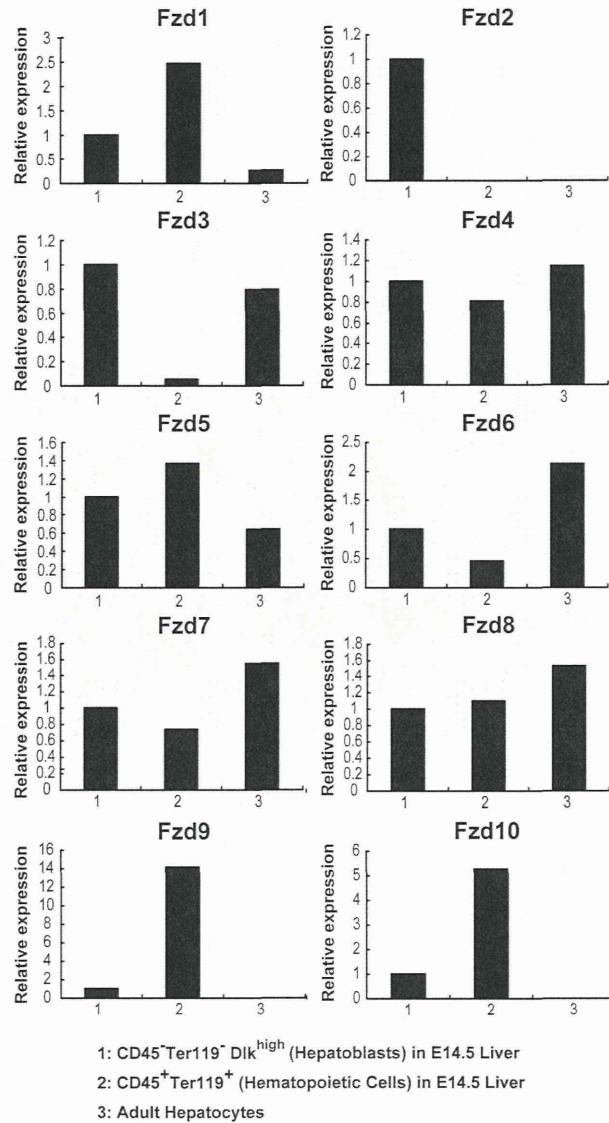
of p-p53/p53 relative to the value in HPPL at pretreatment.

References for supplementary data

1. Kakinuma S, Ohta H, Kamiya A, Yamazaki Y, Oikawa T, Okada K, Nakauchi H. Analyses of cell surface molecules on hepatic stem/progenitor cells in mouse fetal liver. *J Hepatol* 2009;51:127-138.
2. Seglen PO. Hepatocyte suspensions and cultures as tools in experimental carcinogenesis. *J Toxicol Environ Health* 1979;5:551-560.
3. Kakinuma S, Tanaka Y, Chinzei R, Watanabe M, Shimizu-Saito K, Hara Y, Teramoto K, et al. Human umbilical cord blood as a source of transplantable hepatic progenitor cells. *Stem Cells* 2003;21:217-227.
4. Kamiya A, Kakinuma S, Onodera M, Miyajima A, Nakauchi H. Prospero-related homeobox 1 and liver receptor homolog 1 coordinately regulate long-term proliferation of murine fetal hepatoblasts. *Hepatology* 2008;48:252-264.
5. Jenei V, Sherwood V, Howlin J, Linnskog R, Saffholm A, Axelsson L, Andersson T. A t-butylloxycarbonyl-modified Wnt5a-derived hexapeptide functions as a potent antagonist of Wnt5a-dependent melanoma cell invasion. *Proc Natl Acad Sci USA* 2009;106:19473-19478.
6. Tanimizu N, Saito H, Mostov K, Miyajima A. Long-term culture of hepatic progenitors derived from mouse Dlk+ hepatoblasts. *J Cell Sci* 2004;117:6425-6434.
7. Ito T, Udaka N, Yazawa T, Okudela K, Hayashi H, Sudo T, Guillemot F, et al.

Basic helix-loop-helix transcription factors regulate the neuroendocrine differentiation of fetal mouse pulmonary epithelium. *Development* 2000;127:3913-3921.

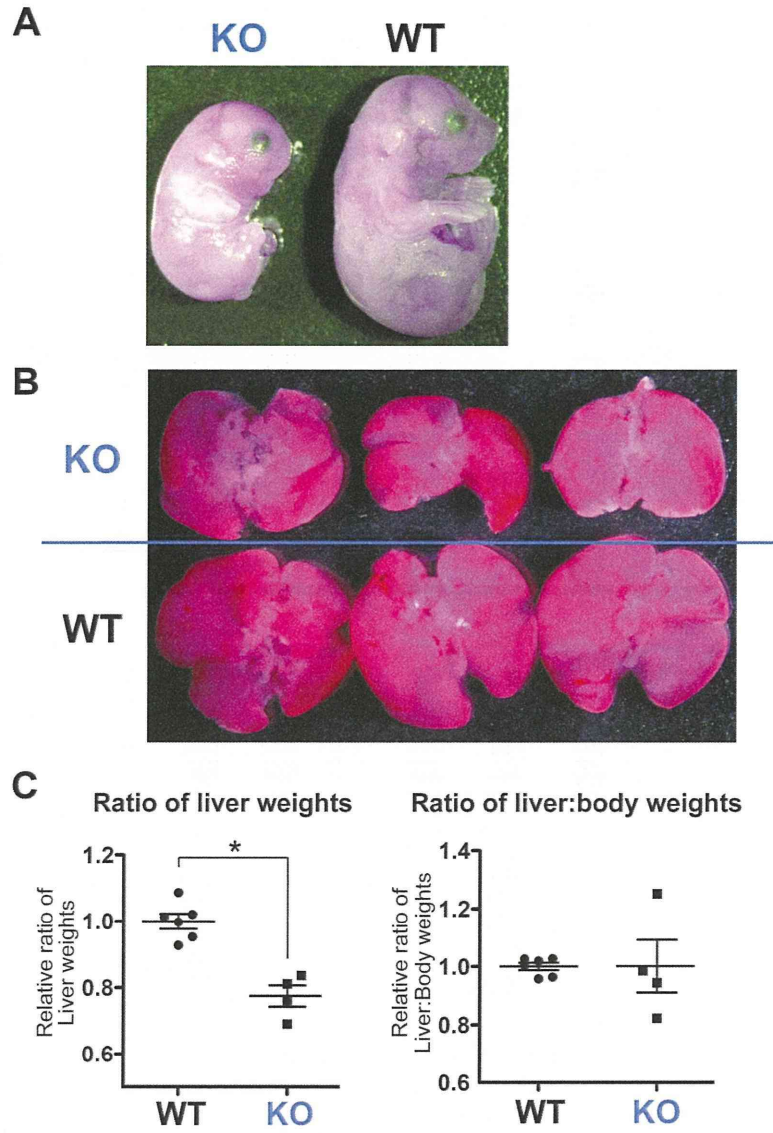
8. Tanimizu N, Miyajima A, Mostov KE. Liver progenitor cells develop cholangiocyte-type epithelial polarity in three-dimensional culture. *Mol Biol Cell* 2007;18:1472-1479.



Kiyohashi *et al.* Supplementary Figure 1

131x251mm (300 x 300 DPI)

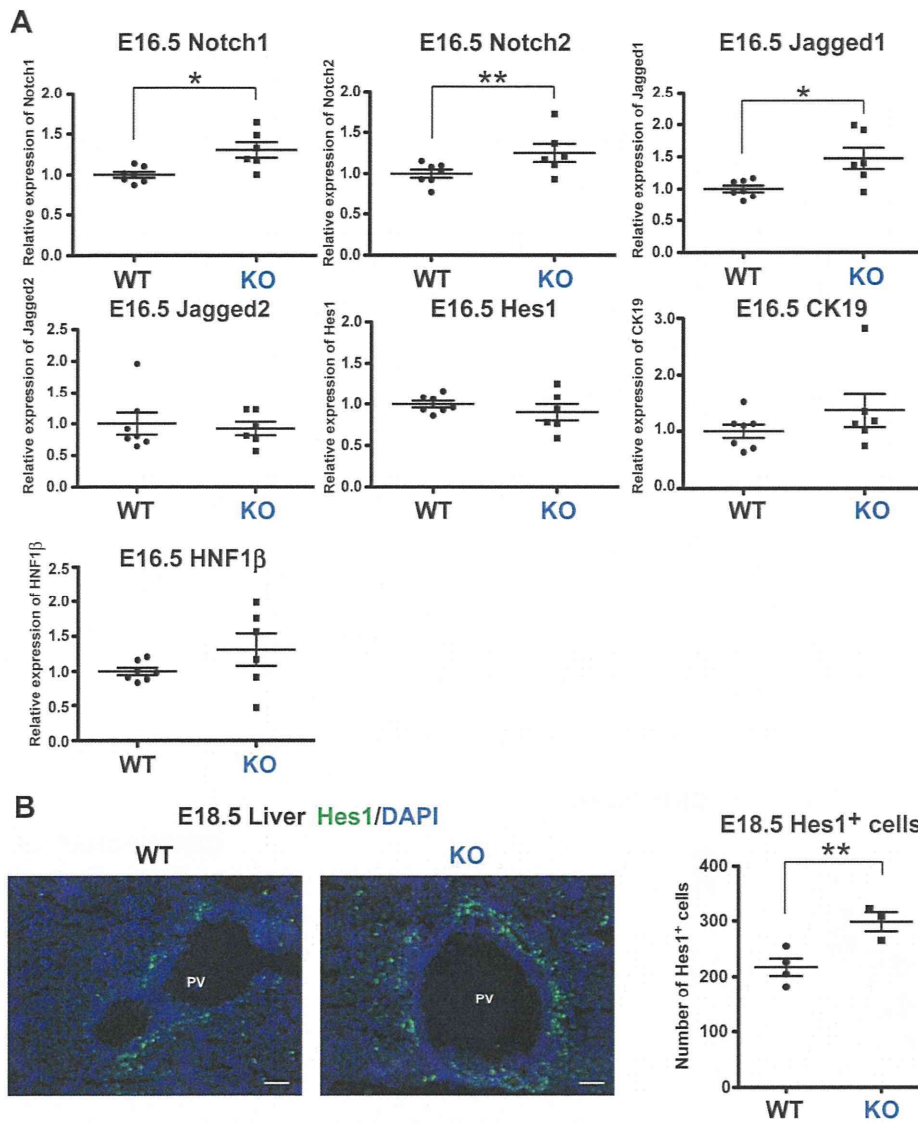
AC



Kiyohashi *et al.* Supplementary Figure 2

174x262mm (300 x 300 DPI)

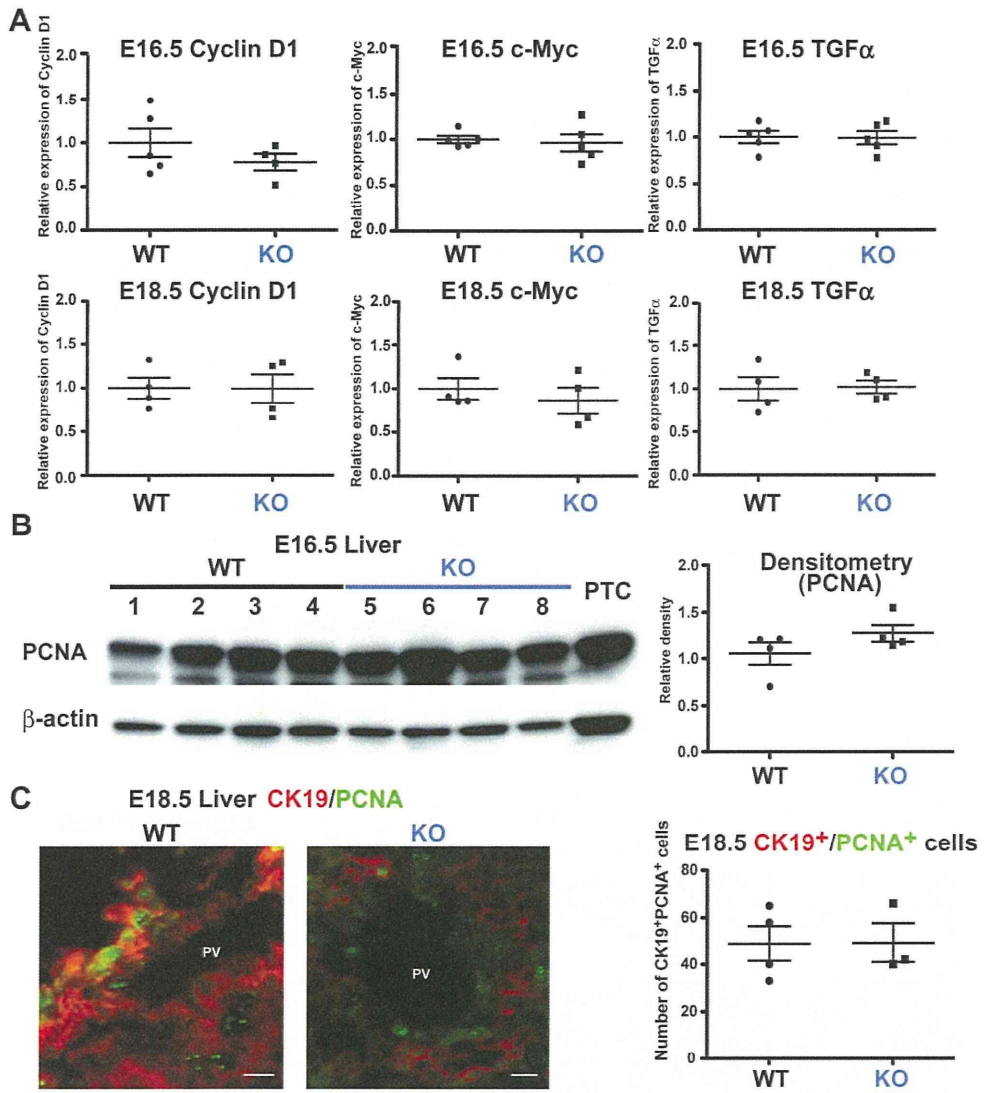
AC



Kiyohashi *et al.* Supplementary Figure 3

203x245mm (300 x 300 DPI)

AC



Kiyohashi *et al.* Supplementary Figure 4

205x239mm (300 x 300 DPI)

AC